

RESEARCH PAPER

Mechanical nanogap switch for low-power on-board electronics

ACHREF YAHIAOUI, EMILIEN LEMOINE, ARNAUD POTHIER AND PIERRE BLONDY

This paper presents the design fabrication and measurement of a nanogap radio frequency microelectromechanical system (RF MEMS) metal-contact switch. The prosed device generates a relatively high contact force with a low actuation voltage using a dielectric layer between the actuation electrode and the moveable beam. The actuation voltage is decreased with good reliability of the device by scaling down the gap. Beam geometry optimization allowed reaching 126 micronewtons contact force with only 10 V bias voltage. The fabricated miniature switch ($80 \times 50 \times 0.95 \mu\text{m}$) has indeed a pull-down voltage of 6 V and a contact resistance $< 2 \Omega$ with 10 V bias applied. By measuring the S-parameters, the up-state capacitance has been fitted to 22 fF. The remarkable figure-of-merit $R_{on} \times C_{up} = 44 \text{ fs}$ reflects the good performance of the device. A cycling test showed the device operated for 90 min without any charging problem noted.

Keywords: RF-MEMS, Nanogaps, Ohmic switches, Low actuation, Miniature

Received 1 January 2014; Revised 28 April 2014; Accepted 15 May 2014; first published online 20 June 2014

1. INTRODUCTION

A major research effort is made to the integration of several functions on the same substrate. Complementary metal-oxide semiconductor (CMOS) integrated circuits have provided an increase in computation speed for several decades [1, 2]. However, the leakage current of the transistor on the off state presents a real limitation for the integration density.

In the other side, the outstanding improvement of microelectromechanical system (MEMS) industrial maturity [3, 4] makes this technology more and more attractive for reconfigurable systems, such as switching networks, portable wireless systems, phased arrays, low-noise oscillators, and amplifiers [1–5]. This is because of the very low loss and the outstanding linearity of radio frequency (RF)-MEMS capacitors arrays [6, 7]. There are several examples of devices with excellent performances in the literature [8–14].

One promising concept is to integrate mechanical switches along with transistors, in the aim to achieve zero off-state power dissipation due to zero leakage current of mechanical switches [7].

However, the successful integration of mechanical switches into CMOS chips requires the pull-down voltage of RF-MEMS to be decreased under 10 V while still maintaining good contact force in the down-state position, since the contact resistance of the switch is directly proportional to this force based on the simplified Hertz contact model.

One possible solution developed in this paper to achieve high electrostatic force with a low actuation voltage, is to

insert a dielectric layer between the actuation electrode and the mobile beam. Indeed, the generated electrostatic force is proportional to the relative permittivity of the media inside the electrostatic gap, as shown in equation (1) [6]:

$$F_e = \frac{\epsilon_r \times \epsilon_0 \times S \times V^2}{2 \times g^2}, \quad (1)$$

where F_e is the electrostatic force, g is the electrostatic gap, V is the applied voltage, S is the surface of the actuator, ϵ_0 is the permittivity, and ϵ_r is the relative permittivity.

Figure 1 shows a conceptual device cross-section with and without dielectric layer between the beam and the actuation electrode.

The electrostatic force is directly proportional to the relative permittivity for a given applied voltage. Moreover, the pull-down voltage is directly proportional to the gap to the power $3/2$.

At the same time, working with low actuation voltage limits dielectric charging issues. This will limit the drift of the actuation voltage over time [6].

$$V_p = \sqrt{\frac{8K}{27 \times \epsilon_0 \times S} \times g_0^3}, \quad (2)$$

Equation (2) illustrates the interest of reducing the initial gap g_0 (the influence of the dielectric layer is neglected for clarity). Indeed, the pull-down voltage is reduced with the initial gap, g_0 , and also it is also possible to increase the switch spring constant K . It means that more force restores the switch to its initial position after bias voltage removal [15]. In addition, the mechanical resonance frequency depends directly on the switch spring constant K and effective

XLIM UMR 7252 – Université de Limoges/CNRS, 123 Avenue Albert Thomas, 87060 Limoges, France

Corresponding author:

A. Yahiaoui

Email: achref.yahiaoui@etu.unilim.fr

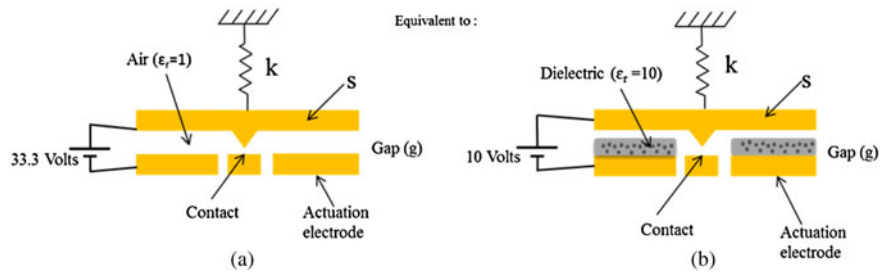


Fig. 1. (a) High actuation voltage with an air-gap (b) low actuation voltage using dielectric layer.

mass m (3) [16, 17]:

$$f_0 = \frac{1}{2\pi} \left(\frac{K}{m} \right)^{(1/2)} \quad (3)$$

This resonance frequency will limit the switching speed of the switch, in fact, to reach a low switching time, the mechanical resonance frequency should be as high as possible [9]. In practice, this means that the device should be as small as possible.

II. SWITCH DESIGN

The miniature switch beam has been designed to be relatively insensitive to structural material built-in stress. It is separated from the actuation electrode by a $0.35 \mu\text{m}$ air-gap and a $0.2 \mu\text{m}$ thin dielectric layer (Fig. 2). In the on-state, the electrostatic force bends the cantilever beam to bring the $0.15 \mu\text{m}$ dimple into contact with the RF line placed on the dielectric layer. Then, as the applied voltage increases, the beam collapses around the dimple on the dielectric layer, providing a better contact force.

The pull-down voltage and the voltage V_2 able to collapse the beam on the dielectric layer are close, since the beam metal thickness is limited. Table 1 summarizes important parameters of the RF-MEMS switch simulated with a finite element method based software, ANSYS.

The metal-contact switch presents two distinct spring constants, K_1 and K_2 , depending on effective metal-to-metal contact. That can be explained by the three phases of switching: the first phase is up-state where the switch presents three anchors with a spring constant K_1 , and the second upon actuation, with four anchors including the dimple, with a spring constant K_2 when the beam collapses on the dielectric layer.

The miniaturization and the round shape of the beam have the purpose of reducing the sensitivity against biaxial built-in stress [18]. In [19], it is shown that the proposed circular design improves the uniformity on a wafer-scale and from wafer-to-wafer lots increasing yield and manufacturability compared to the standard design. In addition, the small size of areas facing each other between the beam and the RF line underneath results in high isolation when the device is in the up state.

III. FABRICATION PROCESS FLOW

Figure 3 details the process flow of the metal-contact switch. The substrate is fused silica for its very low loss performances. The process starts with a first SiCr (50 \AA) metal layer deposition in order to pattern the bottom electrode (a). High resistivity ($> 2 \text{ k}\Omega/\text{sq}$) is sought to minimize current leakage from bias network. Next, a 200-nm thick PVD alumina dielectric ($\epsilon_r = 10$) layer is deposited in order to reach a high electrostatic force on the down state (b). Then, a 100-nm bilayer Ti-Au is evaporated to define contact zone (c). The dimple (150 nm) and the gap (200 nm) are obtained by two successive molybdenum layers depositions (d-e). Then, a last gold layer is evaporated followed by electroplating and definition of the thick cantilever ($0.95 \mu\text{m}$) and the CPW lines (f). Finally, the device is released using a wet etching technique and dried in a CO_2 critical point dryer (g).

IV. ELECTROMAGNETIC ANALYSIS

Figure 4 presents the physical structure of the switch from an electromagnetic perspective and its equivalent circuit model. The total series capacitance between the beam and the RF line is composed of a parasitic series capacitance C_s and the

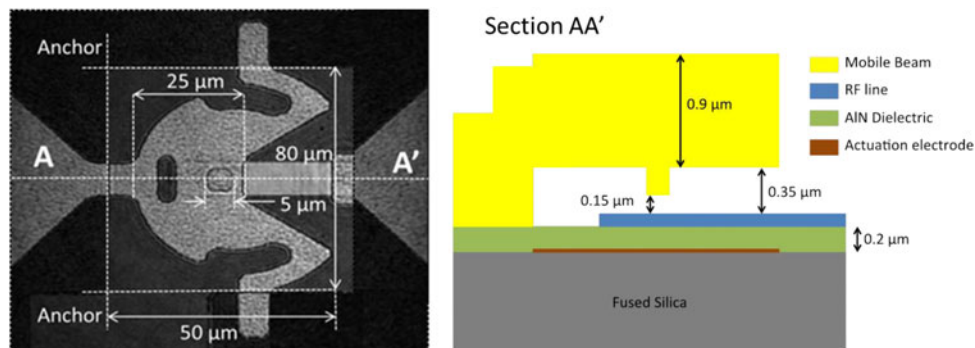
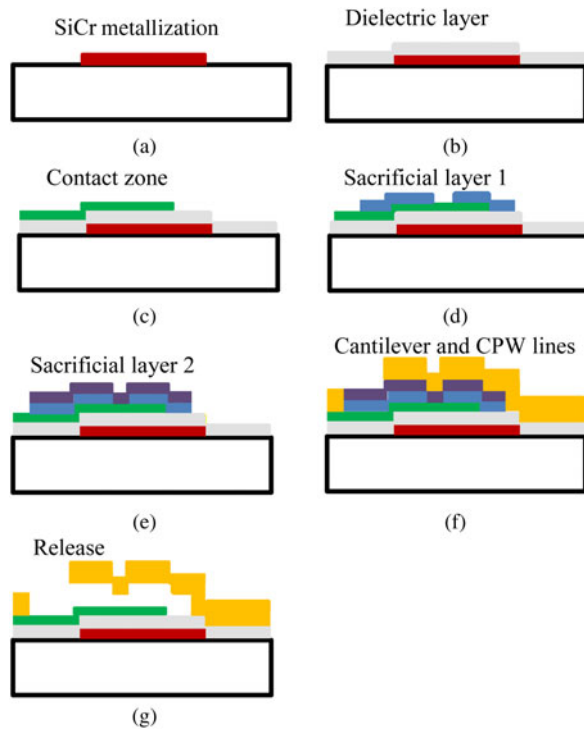


Fig. 2. Optical view and cross-section of the miniature RF MEMS metal-contact switch.

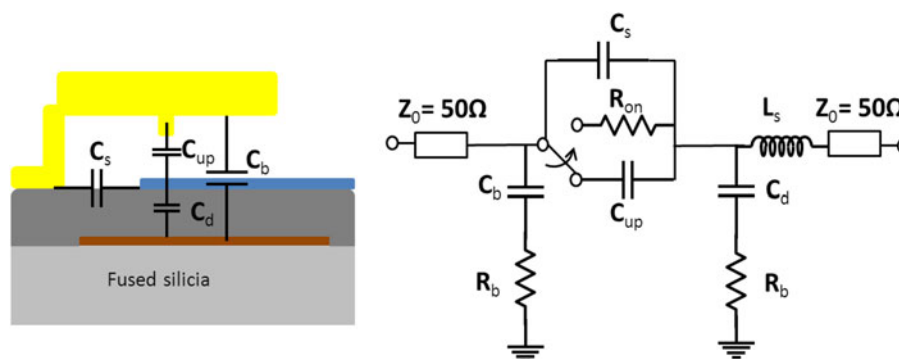
Table 1. Simulated parameters of the metal-contact RF-MEMS switch.

Pull-down voltage (V_p)	6 V
V_2^*	8 V
Resonance frequency (f_0)	300 KHz
Stiffness K_1	60 N/m
Stiffness K_2 (the dimple touches)	200 N/m
Contact force at 10 V	126 μ N
Restoring force	40 μ N

*Voltage able to collapse the beam on the dielectric layer.

**Fig. 3.** Schematic process flow of the MEMS switch.

up-state capacitance C_{up} . C_d is the capacitance between the actuated electrode and the RF line separated by the thin dielectric layer. C_b is the parallel plate capacitance formed between the actuation electrode and the MEMS plate. Since R_b is very large, the bias network has a negligible effect on the RF performance of the device. The element L_s comes from the

**Fig. 4.** Lumped-element model of the RF MEMS contact.

length of the input–output CPW line. R_{on} represents the contact resistance. The different values of the lumped elements are given in Table 2.

V. RF PERFORMANCE AND MEASUREMENT

A) Pull-down and release voltages

An automated test bench with Labview software has been used to measure the behavior of the electromechanical switch. The bench RF system determines the component state by modulating an RF signal by the height of the beam.

The pull-down and release voltages are detected by applying a triangular voltage bias signal. The beam position is known from measurement of the power level detected by a diode at the output of the RF-MEMS.

As it can be seen in Fig. 5, the RF-MEMS switch presents 6 V pull-down voltage and 3 V release voltage. Note that at 8 V, the beam collapses around the dimple.

B) S-parameters

All testing are done on a probe station in a standard laboratory environment without atmosphere or pressure control and with an SOLT calibration planes at AA' (see Fig. 2). Figure 6 presents measured and simulated S-parameters in up and down states position. It shows a high isolation of 30 dB at 2 GHz in the up state. The fitted off capacitance (composed from the C_s in parallel with C_{up}) C_{off} is 22 fF in good agreement very well with Agilent-ADS simulations. When a 10 V bias voltage is applied, the insertion losses are 0.17–0.19 dB and return loss better than 33–35 dB at 2 GHz. The fitted contact resistance R_{on} is $< 2 \Omega$ (Au–Au contact). The insertion loss of 0.17–0.19 dB include both the resistance contact R_{on} and loss of the whole circuit, it is demonstrated by measuring the S-parameters of a switch fabricated on the down state and as a result for that, it presents 0.1 dB of insertion loss. Then, the intrinsic R_{on} contact resistance can be estimated at $< 1 \Omega$.

The figure-of-merit for the RF-MEMS metal-contact switch can be expressed in two ways [20]:

$$f_c = \frac{1}{2\pi \cdot R_{on} \cdot C_{up}} \approx 3.6 \text{ THz}, \quad (4)$$

Table 2. Lumped-element model parameters.

C_{up} (fF)	20
C_s (fF)	2
R_s (Ω)	2
C_d (fF)	43
C_b (fF)	10
R_b (K Ω)	2000
L_s (pH)	170

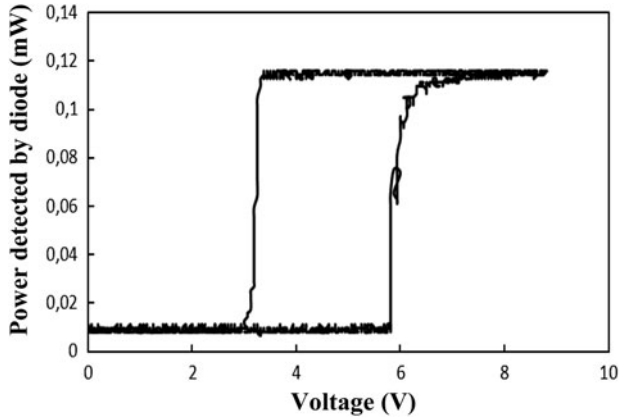


Fig. 5. Pull-down V_p and release voltage V_r of the RF-MEMS switch experimental determination from $P_{detected} = f(V_{bias})$ curve.

$$R_{on} \cdot C_{up} \approx 44 \text{ fs.} \quad (5)$$

The two figures of merit of the resistive switch reflect the good RF performances of the device.

C) Switching time

One of the major advantages of scaling down MEMS cantilevers is significant reduction of effective mass resulting in an increase in the resonant frequency and a decrease in the switching time, even if the control voltage is low. Switching speed measurement has been done using the specific test bench shown in Fig. 7. In this setup, the MEMS component bias signal is generated by a frequency generator and amplified using a wide band high-voltage amplifier. The induced bridge

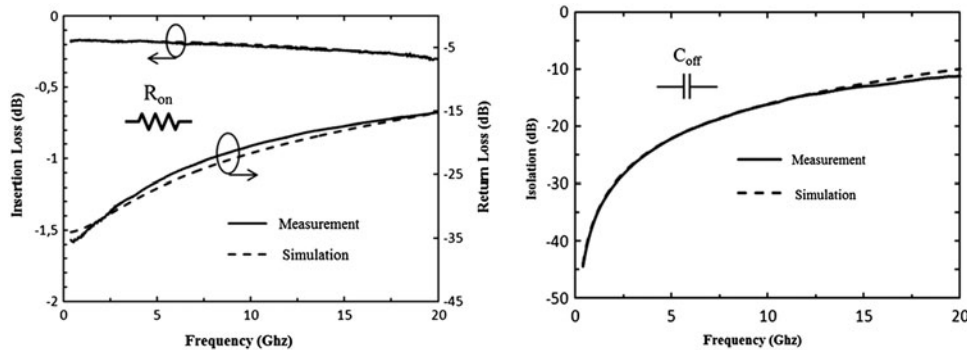


Fig. 6. Measured and simulated S-parameters (a) in down-state position at 10 V and (b) in up-state position.

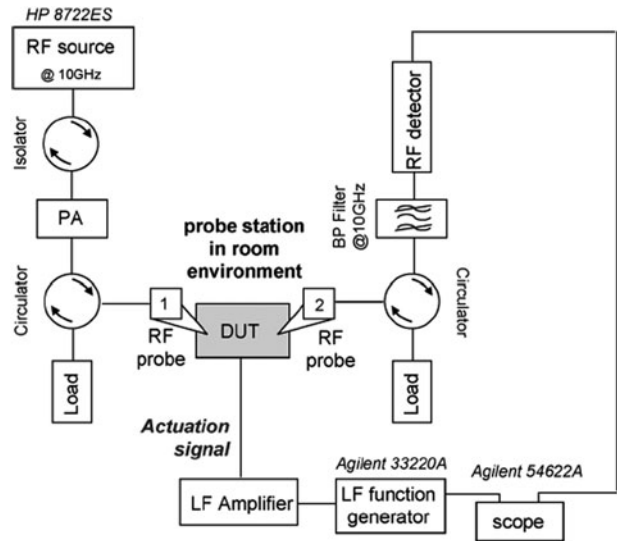


Fig. 7. Switching speed measurement test bench.

motion over time can be detected by measuring the amount of RF signal reflected at the component input. This reflected signal is collected by a circulator, and then sent to a diode detector, and the bridge displacement can be detected using an oscilloscope. A wideband power meter with 8 ns resolution completes this test setup to accurately detect the beam switching delay compared to the actuation signal. MEMS structures have been tested under vacuum and actuated using a 10 kHz bipolar signal in order to limit dielectric charging issue and ensure time stable measurement. Switching speed measurement has been done for different actuation voltages. For an 8 V bias voltage, the switching time is 9 μ s, and then as the applied voltage increases, the switching time decreases substantially to reach 4.5 μ s at 11 V bias voltage as shown in Fig. 8.

The bouncing shown in Fig. 8 could be explained by the fact that the measurements are done in vacuum environment.

VI. RELIABILITY

The sensitivity of the device to dielectric charging has been tested using an automated test bench that records pull-in and pull-out voltages automatically. The MEMS device is left in the down state with 10 V (DC) applied and the

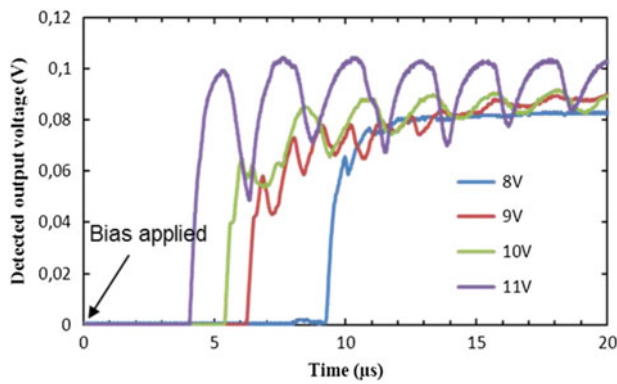


Fig. 8. Switching time for different applied bias voltages.

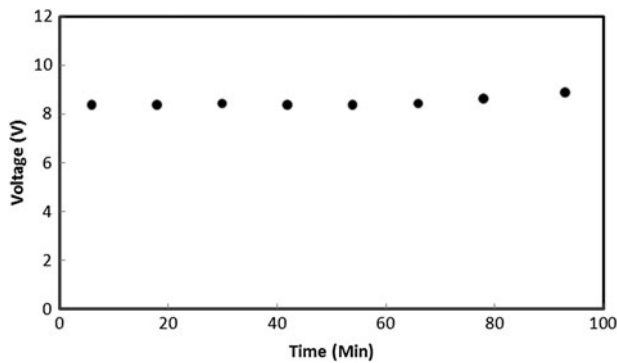


Fig. 9. Evolution of V_p over time.

pull-in and pull-out voltages are recorded every 3 s. The tests were conducted in vacuum and the results are plotted in Fig. 9.

It can be seen that the pull-in voltage has a very small evolution over time, from an initial value of 8.5 V, up to 9 V after 90 min. No specific optimization was done on the dielectric layer and the results are showing the small sensitivity of these devices to charge retention.

VII. CONCLUSIONS

This paper presents a new concept of metal-contact RF-MEMS switch using nanometer electrostatic gaps. The deposition of a dielectric layer allows achieving a relatively large electrostatic force in the down-state position for a given voltage. The pull-down voltage can be reduced substantially (below 10 V) by scaling down the gap and still ensuring a good contact force. The concept was validated by measuring the insertion loss on the down-state position which was below 0.2 dB at 2 GHz. The effective contact resistance is approximated to $< 2 \Omega$, resulting in a 44 fs figure-of-merit. Moreover, scaling down the gap permits reducing the pull-down voltage further and increase the stiffness of the device. It was demonstrated also that by having a low pull-down voltage, the charge retention issues are minimized, through pull-in voltage measurements.

Work is on-going in our laboratory for reliability testing and power-handling. In a long-term view, further miniaturization and integration into CMOS circuits will be conducted.

REFERENCES

- [1] Rebeiz, G.M.; Muldavin, J.B.: RF MEMS switches and switch circuits. *IEEE Microw. Mag.*, **2** (4) (2001), 59–71.
- [2] Xu, J.; Chowdhury, M.H.: Latch based interconnect pipelining for high speed integrated circuits, in 2006 IEEE Int. Conf. on Electro/Information Technology, 2006, 295–300.
- [3] Morris wiSpry, A.: Tunable RF modules for mobile applications, in IMS Emerging Application of RF MEMS Workshop, 2009.
- [4] Meindl, J.D.; Chen, Q.; Davis, J.A.: Limits on silicon nanoelectronics for terascale integration. *Science*, **2044** (9) (2001), 293.
- [5] Pethica, J.; Tabor, D.: Contact of characterised metal surfaces at very low loads: deformation and adhesion. *Surface Sci.*, **89** (1979), 182–190.
- [6] Rebeiz, G.M.: RF MEMS Theory, Design, and Technology, J. Wiley & Sons, New Jersey, 2003.
- [7] Newman, H.S.; Ebel, J.L.; Judy, D.; Maciel, J.: Lifetime measurements on a high-reliability RF-MEMS contact switch. *IEEE Microw. Wirel. Compon. Lett.*, **18** (2) (2008), 100–102.
- [8] Nishijima, N.; Hung, J.-J.; Rebeiz, G.M.: Parallel-contact metal-contact RF-MEMS switches for high power applications, in 17th IEEE Int. Conf. on Micro Electro Mechanical Systems, 2004. (MEMS), 2004, 781–784.
- [9] Oberhammer, J.; Stemme, G.: Low-voltage high-isolation DC-to-RF MEMS switch based on an S-shaped film actuator. *IEEE Trans. Electron Devices*, **51** (1) (2004), 149–155.
- [10] Sedaghat-Pisheh, H.; Rebeiz, G.M.: Variable spring constant, high contact force RF MEMS switch, in 2010 IEEE MTT-S Int. Microwave Symp. Digest (MTT), 2010, 1–1.
- [11] Reines, I.C.; Rebeiz, G.M.: A robust high power-handling (> 10 W) RF MEMS switched capacitor, in 2011 IEEE 24th Int. Conf. on Micro Electro Mechanical Systems (MEMS), 2011, 764–767.
- [12] Goggin, R.; Wong, J.-E.; Hecht, B.; Fitzgerald, P.; Schirmer, M.: Fully integrated, high yielding, high reliability DC contact MEMS switch technology amp; control IC in standard plastic packages, in 2011 IEEE Sensors, 2011, 958–961.
- [13] Menz, A.; Hoper, R.: Micromechanical silicon RF switch with electroplated solid contacts for high reliability, in Seventh European Microwave Integrated Circuits Conf. (EuMIC 2012), 2012, 453–456.
- [14] Ke, F.; Miao, J.; Oberhammer, J.: A ruthenium-based multimetal-Contact RF MEMS switch with a corrugated diaphragm. *J. Microelectromechanical Syst.*, **17** (6) (2008), 1447–1459.
- [15] Patel, C.D.; Rebeiz, G.M.: An RF-MEMS switch with mN contact forces, in 2010 IEEE MTT-S Int. Microwave Symp. Digest (MTT), 2010, 1–1.
- [16] Lakshminarayanan, B.; Mercier, D.; Rebeiz, G.M.: High-reliability miniature RF-MEMS switched capacitors. *IEEE Trans. Microw. Theory Tech.*, **56** (4) (2008), 971–981.
- [17] Verger, A.; et al.: Sub-hundred nanosecond reconfiguration capabilities of nanogap RF MEMS switched capacitor, in 2010 IEEE MTT-S Int. Microwave Symp. Digest (MTT), 2010, 1–1.
- [18] Rebeiz, G.M.: Phase-noise analysis of MEMS-based circuits and phase shifters. *IEEE Trans. Microw. Theory Tech.*, **50** (5) (2002), 1316–1323.
- [19] Reines, I.; Pillans, B.; Rebeiz, G.M.: A stress-tolerant temperature-stable RF MEMS switched capacitor, in IEEE 22nd Int. Conf. on Micro Electro Mechanical Systems, 2009. (MEMS 2009), 2009, 880–883.
- [20] Stefanini, R.; Chatras, M.; Blondy, P.; Rebeiz, G.M.: Miniature RF MEMS metal-contact switches for DC-20 GHz applications, in 2011 IEEE MTT-S Int. Microwave Symp. Digest (MTT), 2011, 1–4.



Achref Yahiaoui received the Master's degree in circuits, systems, and micro and nanotechnology for optical and high-frequency communications from the University of Limoges, Limoges, France. He is currently toward the Ph.D. degree in high frequency communications in the XLIM laboratory, University of Limoges. He served a

6-month internship in the Electrical and Computer Engineering Department of the University of California at San Diego, La Jolla. His research interests include microelectromechanical systems devices.



Emilien Lemoine received the Master's degree in Circuits, Systems, and Micro and Nanotechnology for optical and high frequencies telecommunications in 2011 from University of Limoges in France. He is currently toward the Ph.D. degree in reliability of RF MEMS in Xlim laboratory in the University of Limoges, Limoges, France.



Arnaud Pothier received the Ph.D. degree in Electrical Engineering from the University of Limoges, Limoges, France, in 2003. He is currently a Full-Time Researcher with the Centre National de la Recherche Scientifique (CNRS), XLIM, University of Limoges. His current research activity is focused on the tunability functions development

and implementation for analogical communication modules using RF MEMS components especially for reconfigurable/programmable filters and phase shifters.



Pierre Blondy (M'99) received the Ph.D. and Habilitation degrees from the University of Limoges, Limoges, France, in 1998 and 2003, respectively. From 1998 to 2006, he was with the Centre National de la Recherche Scientifique, as a Research Engineer with the Xlim Laboratory, where he began research on radio frequency microelectromechanical system (RF MEMS) technology and applications to microwave circuits. He is currently a Professor at the University of Limoges, leading a research group on RF MEMS and he is holding an Institut Universitaire de France chair, to conduct research on innovative microwave circuits. He was a Visiting Researcher at the University of Michigan, Ann Arbor, in 1997, and at the University of California at San Diego, La Jolla, in 2006 and 2008. He has authored or co-authored more than 150 papers in refereed journals and conferences proceedings. Dr. Blondy was an Associate Editor for the IEEE MICROWAVE AND WIRELESS COMPONENTS LETTERS in 2006. He has been a member of the IEEE International Microwave Conference Technical Program Committee since 2003. He was the recipient of the MTT-S "Outstanding Young Engineer Award" in 2011 for his research on RF MEMS.

and applications to microwave circuits. He is currently a Professor at the University of Limoges, leading a research group on RF MEMS and he is holding an Institut Universitaire de France chair, to conduct research on innovative microwave circuits. He was a Visiting Researcher at the University of Michigan, Ann Arbor, in 1997, and at the University of California at San Diego, La Jolla, in 2006 and 2008. He has authored or co-authored more than 150 papers in refereed journals and conferences proceedings. Dr. Blondy was an Associate Editor for the IEEE MICROWAVE AND WIRELESS COMPONENTS LETTERS in 2006. He has been a member of the IEEE International Microwave Conference Technical Program Committee since 2003. He was the recipient of the MTT-S "Outstanding Young Engineer Award" in 2011 for his research on RF MEMS.